

Neural MOS Prediction for Synthesized Speech Using Multi-Task Learning With Spoofing Detection and Spoofing Type Classification

Yeunju Choi, Youngmoon Jung, Hoirin Kim

School of Electrical Engineering, KAIST, Daejeon, Republic of Korea

{wkadldppdy, dudans, hoirkim}@kaist.ac.kr

Abstract

Several papers have proposed deep-learning-based models to predict the mean opinion score (MOS) of synthesized speech, showing the possibility of replacing human raters. However, inter- and intra-rater variability in MOSs makes it hard to ensure the generalization ability of the models. In this paper, we propose a method using multi-task learning (MTL) with spoofing detection (SD) and spoofing type classification (STC) to improve the generalization ability of a MOS prediction model. Besides, we use the focal loss to maximize the synergy between SD and STC for MOS prediction. Experiments using the results of the Voice Conversion Challenge 2018 show that proposed MTL with two auxiliary tasks improves MOS prediction.

Index Terms: speech synthesis, MOS prediction, multi-task learning, spoofing detection, spoofing type classification

1. Introduction

Speech generation tasks such as text-to-speech and voice conversion have achieved great success in recent years with advances in deep learning [1–5]. In terms of the quality of synthesized speech, state-of-the-art systems have reached human-level performance. However, researchers still rely on a subjective mean opinion score (MOS) test to evaluate the quality of the synthesized speech. Researchers need to employ enough human raters and give them a guideline to evaluate synthesized utterances, which is expensive and time-consuming [6]. Additionally, different studies may produce inconsistent results when evaluating the same speech generation system.

Therefore, researchers have recently proposed deep-learning-based models to predict the subjective MOS of synthesized speech [7–9]. Patton *et al.* [8] proposed AutoMOS, based on long short-term memory (LSTM), to predict the MOS. Lo *et al.* [9] proposed MOSNet based on convolutional neural network-bidirectional LSTM (CNN-BLSTM), which produces an utterance-level MOS using frame-level scores. Furthermore, to evaluate and compare the performance of systems, a system-level MOS is calculated by averaging utterance-level MOSs.

However, inter- and intra-rater variability of MOSs fundamentally limits the generalization ability of the predictor. We expect that multi-task learning (MTL) [10, 11], a famous regularization technique, can alleviate the problem. MTL helps a model to generalize better by using the information in related tasks, which are used as auxiliary tasks for the main task. It has been successfully applied to various research areas [12–17].

As suggested by [18], identifying beneficial auxiliary tasks is important in MTL. For example, for slot filling in language understanding, [19] proposed to use named entity recognition as an auxiliary task. In this work, we propose to apply MTL with spoofing detection (SD) and spoofing type classification (STC) to help MOS prediction. To the best of our knowledge, this is the first work that uses MTL for MOS prediction. We

also present a detailed analysis of the effect of our approach. Besides, we use the focal loss [20] for SD to improve our MTL approach. Experiments using the evaluation results of the Voice Conversion Challenge (VCC) 2018 show that both auxiliary tasks help MOS prediction. They also demonstrate that SD can create more synergy with STC by using the focal loss.

2. Proposed methodology

2.1. MOS prediction model

For MOS prediction, we adopt the recently proposed MOSNet [9] that predicts the MOS of synthesized speech with a deep neural network using a large open dataset. In [9], three different architectures were proposed: CNN, BLSTM, and CNN-BLSTM. Among them, we use the CNN-BLSTM-based MOSNet as our baseline model since it achieved the best results.

The architecture of the model is shown in gray in Fig. 1. The input and output of MOSNet are a 257-dimensional magnitude spectrogram and a MOS of an utterance, respectively. First, the CNN-BLSTM network extracts frame-level features. The following two fully-connected (FC) layers predict frame-level scores from the frame-level features. Finally, we obtain the utterance-level MOS by averaging the frame-level scores.

The overall loss function is as follows:

$$L = \frac{1}{U} \sum_{u=1}^U [(\hat{Q}_u - Q_u)^2 + \frac{\alpha_f}{T_u} \sum_{t=1}^{T_u} (\hat{Q}_u - q_{u,t})^2], \quad (1)$$

where the first and second terms are mean squared errors (MSEs) for the utterance-level MOS and frame-level MOS, respectively. u is an utterance index, and U is the number of training utterances. \hat{Q}_u and Q_u are the ground-truth MOS and predicted MOS for the u -th utterance, respectively. t is a frame index, and T_u is the length of the u -th utterance. $q_{u,t}$ is the predicted frame-level MOS at the t -th frame of the u -th utterance. α_f is a loss weight for frame-level MOS prediction.

2.2. Multi-task learning setup

To improve MOS prediction, we propose MTL with two auxiliary tasks: spoofing detection (SD) and spoofing type classification (STC). In this work, SD refers to a task to classify human speech as “human” and synthesized speech as “spoofing” [21]. STC is a task to identify the source of input speech, which can be a speech generation system or a human speaker. Since the synthesized speech is used for spoofing, we call the speech generation system a “spoofing system,” and all the spoofing systems and human speakers are collectively called “spoofing types.”

Fig. 1 shows the architecture of our MTL model where 14 layers are shared by all the tasks, consisting of the CNN-BLSTM network and FC layer with 128 nodes (FC-128). For MOS prediction, the FC-1 layer is used to predict frame-level

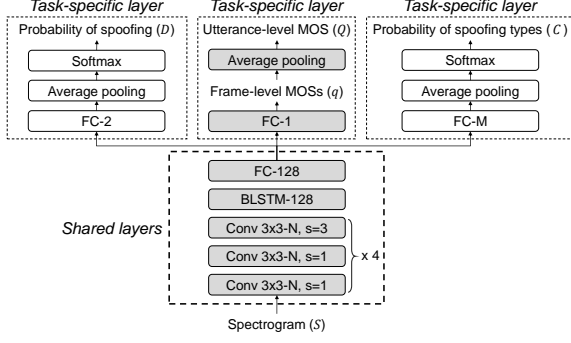


Figure 1: Overview of the proposed model. The MOS prediction model is shown in gray. N is the number of channels of three convolution layers, corresponding to 16, 16, 32, and 32 for four stacks. M : number of spoofing types, s : stride of convolution.

MOSs, and the following average pooling layer is used to predict the utterance-level MOS. For each auxiliary task, we assign an additional task-specific layer, which consists of FC, average pooling, and softmax layers. The number of nodes of the FC layer is the same as the number of classes for each task, i.e., 2 for SD, and the number of spoofing systems plus 2 (corresponding to the source and target speakers) for STC.

We use the cross-entropy loss for both auxiliary tasks. Then we define the final loss function as follows:

$$L = \frac{1}{U} \sum_{u=1}^U [\alpha_m (\hat{Q}_u - Q_u)^2 + \frac{\alpha_f}{T_u} \sum_{t=1}^{T_u} (\hat{Q}_u - q_{u,t})^2 - \alpha_d \sum_{i=1}^2 \hat{D}_{u,i} \log D_{u,i} - \alpha_c \sum_{j=1}^M \hat{C}_{u,j} \log C_{u,j}], \quad (2)$$

where $\hat{D}_{u,i}$ and $D_{u,i}$ are the i -th dimension of the ground-truth and predicted probability of spoofing for the u -th utterance, respectively. $\hat{C}_{u,j}$ and $C_{u,j}$ are the ground-truth and predicted probability of j -th spoofing type for the u -th utterance, respectively. M is the number of spoofing types. α_m , α_d , and α_c are the loss weights for utterance-level MOS prediction, SD, and STC, respectively. In this setup, the number of parameters only increases by 1.438% (from 358,833 to 363,993).

2.3. Analysis of auxiliary tasks for MOS prediction

Fig. 2 is a conceptual illustration of the decision boundary in the SD task that separates the shared features of human speech and spoofed (or synthesized) speech, which are extracted from the shared layers. From now on, we give a detailed analysis of the proposed MTL approach based on this figure.

We first discuss the difficulty of MOS prediction, especially for high MOS. Human speech usually has higher MOS than synthesized speech, as also can be seen in Fig. 3. Among the synthesized utterances, there are much fewer utterances with high MOSs (i.e., high-quality speech) than those with low MOSs (i.e., low-quality speech), which makes it difficult for a MOS prediction model to predict high MOSs. We show that using the SD task can alleviate this problem.

In SD, the model is trained to discriminate between human speech and synthesized speech. Then it learns a decision boundary in a zone marked as ‘‘Concentrating effect zone’’ in Fig. 2, where both human speech and high-quality synthesized speech exist. Therefore, if we train a model on the SD task, the model can learn to distinguish between the human speech and high-

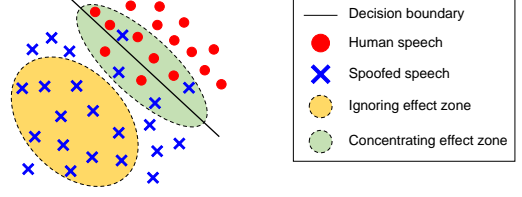


Figure 2: A conceptual illustration of decision boundary in SD.

quality synthesized speech by giving more attention to high-quality speech than when trained only on MOS prediction. As a result, in MOS prediction, the model will predict high MOSs better by concentrating on the utterances with high MOSs. Accordingly, we call the effect above *concentrating effect*.

As discussed in Section 2.2, in STC, the model is trained to identify the source of speech, called the spoofing type, and thus learns low-level features that are useful for distinguishing between various types of speech. Here, the spoofing type fundamentally determines the way of vocalization and intonation, which has a large effect on the MOS of speech. In addition to these reasons, we believe that the independence of these two tasks from the raters may be helpful for inter- and intra- rater variability. Experimental results in Section 4 support the effectiveness of using these auxiliary tasks.

2.4. Focal loss for the spoofing detection task

In this section, we describe our motivation to use the focal loss for SD. The SD model is trained to classify synthesized utterances into the same class, ‘‘spoofing,’’ even though the utterances are generated by various spoofing systems. Then MTL with SD would prevent the model from distinguishing between spoofing systems. We call this effect of SD *ignoring effect* as it ignores the difference between unique spoofing systems.

However, when we train a MOS predictor with STC, the model will be able to distinguish between the spoofing types in training data, which we call *distinguishing effect*. Then, when testing the model using the same spoofing types in training data, using SD as another auxiliary task causes a conflict between the *ignoring effect* and *distinguishing effect*. To maximize the synergy between SD and STC, we want to prevent SD from having the *ignoring effect*. Note that there are much more synthesized utterances far from the decision boundary, having lower MOSs and SD losses, than those near the decision boundary, having higher MOSs and SD losses (see Fig. 2). Those low-quality synthesized utterances having low SD losses contribute to only the *ignoring effect* but not the *concentrating effect*, marked as ‘‘Ignoring effect zone.’’ To reduce the contribution of the utterances with low SD losses, we adopt the focal loss [20] for SD.

The cross-entropy (CE) loss of the u -th utterance for the SD task is as follows:

$$CE(D_u, \hat{D}_u) = \begin{cases} -\log D_{u,1}, & \text{if } \hat{D}_u = (1, 0) \\ -\log D_{u,2}, & \text{if } \hat{D}_u = (0, 1). \end{cases} \quad (3)$$

The first and second dimensions of \hat{D}_u corresponds to the ‘‘human’’ and ‘‘spoofing,’’ respectively. Please note that $D_{u,2} = 1 - D_{u,1}$ since we use the softmax layer.

Now we define $p_u \in [0, 1]$ as follows for convenience:

$$p_u = \begin{cases} D_{u,1}, & \text{if the } u\text{-th utterance} \in \text{‘‘human.’’} \\ 1 - D_{u,1}, & \text{otherwise.} \end{cases} \quad (4)$$

Then the CE loss can be rewritten as $CE(p_u) = -\log(p_u)$. To down-weight the contribution of easy samples (that have lower

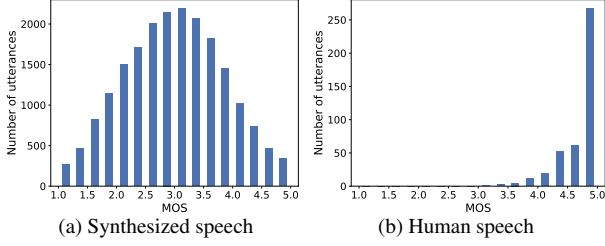


Figure 3: Distribution of ground-truth utterance-level MOSs for (a) synthesized and (b) human speech from the VCC’18 data.

loss) and focus on hard samples (that have higher loss), the focal loss (FL) is defined as $FL(p_u) = -(1 - p_u)^\gamma \log(p_u)$ with a parameter $\gamma \geq 0$ that adjusts the rate at which easy samples are down-weighted.

3. Experiments

3.1. Dataset

We use the MOS evaluation results of the VCC 2018 (VCC’18) [22], which is a large, open, and intrinsically-predictable dataset. A total of 38 systems participated in VCC’18, including two human speakers (target and source speakers). The ground-truth MOS of a system was obtained by averaging the ground-truth MOSs of all the utterances from the system.

A total of 267 people rated a total of 20,580 utterances on a scale of 1 (completely unnatural) to 5 (completely natural). An average of 4 people per utterance participated in the evaluation, leading to a total of 82,304 evaluation results. The ground-truth of the utterance-level MOS was obtained as the average of all the MOSs of the utterance. Fig. 3 shows the distribution of ground-truth utterance-level MOSs. From 20,580 <audio, ground-truth MOS > pairs, we randomly select 15,580, 3,000, and 2,000 pairs for training, validation, and testing, respectively.

We also use the MOS evaluation data from the VCC 2016 (VCC’16) [23] to evaluate the robustness of the models to unseen spoofing types and raters. Including a target speaker, source speaker, and baseline system, a total of 20 systems exist. For each system, 1,600 utterance-level evaluation results exist with no specification of the utterances or raters. Therefore, we cannot use the utterance-level MOSs and only use the system-level MOSs with a total of 26,028 utterances.

3.2. Implementation details

All the models are implemented using PyTorch and trained on a single GTX 1080 Ti GPU. We use a batch size of 32 and the Adam optimizer with a learning rate of 10^{-4} for all the models. We set the weights for utterance- and frame-level MOS prediction to 1 and 0.8, respectively. For MTL, we set the weight of the loss for each auxiliary task to 1. When we adopt the focal loss (FL) for the SD task, we set γ to 0.8.

For testing, we use the model that has the lowest MSE on the VCC’18 validation set during 200 epochs of training. Note that we train all the models using only the VCC’18 training set and test them on both the VCC’18 test set and VCC’16 data. We conduct the experiments for each model with four different random seeds and report the average value of the four results as the performance of each model. The performance is evaluated in terms of the MSE, linear correlation coefficient (LCC) [24], and Spearman’s rank correlation coefficient (SRCC) [25]. We report both utterance- and system-level performances for the VCC’18 test set. For the VCC’16 data, we report only system-level per-

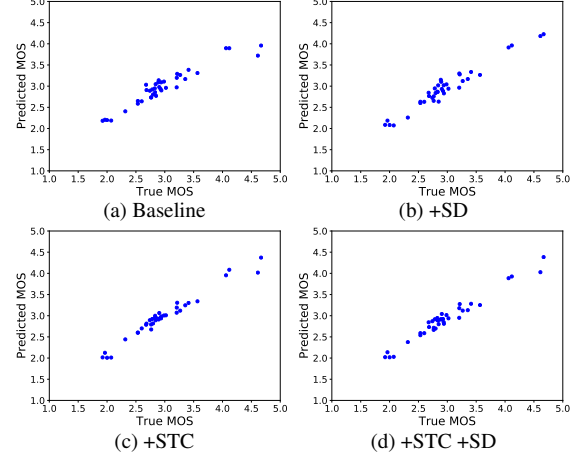


Figure 4: Scatter plots of system-level MOSs for (a) Baseline, (b) MTL model with SD (+SD), (c) MTL model with STC (+STC), and (d) MTL model with both tasks (+STC +SD).

formance because the utterance-level MOSs for the VCC’16 are not available, as mentioned in Section 3.1.

4. Results and Discussion

4.1. Effectiveness of auxiliary tasks

Table 1 shows the effectiveness of the proposed MTL approach. The results of MTL with SD (+SD) and STC (+STC) are in the second and fourth rows of Table 1, respectively. +SD improved the baseline in terms of all the metrics with the VCC’18 data. Moreover, +STC achieved better performance compared to the baseline, not only on the VCC’18 data but also on the VCC’16 data. +STC yielded better results than +SD, which corresponds to the intuition that the model learns more information with a multi-class classification task (i.e., STC) than with a simple binary classification task (i.e., SD).

The MTL model with both auxiliary tasks (+STC +SD) improved the performance of the baseline in terms of all the metrics except the utterance-level SRCC for the VCC’18, which is almost the same as the baseline. However, the performance on the VCC’18 data was not better than that of +STC due to the conflict between the *ignoring effect* and *distinguishing effect*. In Section 4.3, we will see that the focal loss reduces the *ignoring effect*, and thus improves the performance of +STC +SD.

Fig. 4 shows the scatter plots of system-level MOSs for four models. Each dot corresponds to individual system. Comparing (a) and (b), we can see that the systems with high MOSs are better aligned using MTL with SD. This indicates that using SD is useful for MOS prediction in high MOS, as discussed in Section 2.3. Comparing (a) and (c), we can see that the dots get closer to the $y = x$ line using MTL with STC, which means that predicted MOSs are more close to ground-truth MOSs. The scatter plot of system-level MOSs for +STC +SD, shown in (d), looks like the combination of (b) and (c).

4.2. Generalization to unseen spoofing types and raters

As mentioned in the introduction, inter- and intra- rater variability exists in MOSs. Different raters evaluate speech quality based on their own subjectivity without objective criteria, leading to high variance within the evaluated scores of the same speech [9]. This variability caused by the raters fundamentally limits the generalization ability of a MOS predictor.

As spoofing types and raters are not overlapping between

Table 1: Results of ablation study. MOS and F-MOS are utterance- and frame-level MOS, respectively. +SD and +STC denote using the SD and STC task, respectively. RI is the average relative improvement of nine metrics. The best results are shown in bold.

Model	FL	Loss weights				VCC'18						VCC'16			RI (%)
		α_m (MOS)	α_f (F-MOS)	α_d (SD)	α_c (STC)	utterance-level			system-level			system-level			
						MSE	LCC	SRCC	MSE	LCC	SRCC	MSE	LCC	SRCC	
Baseline	-	1	0.8	0	0	0.448	0.651	0.619	0.039	0.966	0.924	0.316	0.896	0.858	-
+SD	-	1	0.8	1	0	0.439	0.661	0.623	0.029	0.972	0.925	0.333	0.886	0.829	2.34
+SD	✓	1	0.8	1	0	0.445	0.655	0.621	0.029	0.971	0.934	0.283	0.907	0.847	4.31
+STC	-	1	0.8	0	1	0.434	0.666	0.625	0.020	0.982	0.955	0.226	0.915	0.859	10.2
+STC +SD	-	1	0.8	1	1	0.435	0.664	0.618	0.019	0.983	0.944	0.227	0.925	0.883	10.5
+STC +SD	✓	1	0.8	1	1	0.431	0.668	0.622	0.016	0.985	0.944	0.208	0.904	0.864	11.6

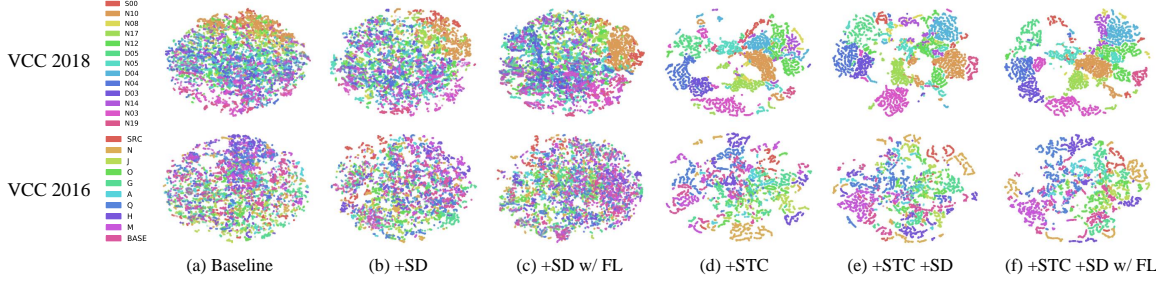


Figure 5: *t*-SNE plots of shared features of six different models. The legends are sorted in descending order based on system-level MOS.

the VCC'16 and 18, we can see the generalization ability of the models to unseen spoofing types and raters from the test results on the VCC'16 in Table 1. +SD degrades the performance of the baseline on the VCC16 since it tends to prevent the model from distinguishing between spoofing systems by the *ignoring effect* while there are more variations in spoofing systems in the VCC'16; the ground-truth system-level MOSs of the spoofing systems have a higher standard deviation in the VCC'16 (0.59) than in the VCC'18 (0.49).

Meanwhile, we can see that +STC shows better generalization ability than the baseline on the VCC'16. We argue that it is because, in the process of distinguishing various systems, the shared layers learn useful low-level features that can be generalized to unseen spoofing types and raters. Moreover, by using the SD task to +STC, +STC +SD achieves a 10% relative improvement compared to +STC on the VCC'16 data. We provide a detailed analysis of the result in Section 4.4.

4.3. Effect of the focal loss for spoofing detection

As discussed in Section 2.4, if we use the FL for SD in training, a model tends to keep learning from the utterances with high SD losses but to stop learning from those that have relatively low SD losses. That is, the FL increases the *concentrating effect* and decreases the *ignoring effect* on SD. For the VCC'18 test set, +SD w/ FL plays a similar role with +SD in terms of that it helps MOS prediction by the *concentrating effect*. For the VCC'16 data, however, it improved +SD by relieving the *ignoring effect* that acted as a disadvantage for +SD, as we discussed in Section 4.2. Applying the FL to +STC +SD improved the performance for the VCC'18 test set by relieving the *ignoring effect* that limited the performance of +STC +SD. For the VCC'16 data, +STC +SD w/ FL achieved little better than +STC +SD. In summary, +STC +SD w/ FL achieved the best relative improvement of 11.6% compared to the baseline.

4.4. Visualization of shared features

To further support our analysis, we visualized the shared features using t-distributed stochastic neighbor embedding (t-SNE) [26] in Fig. 5. We displayed a frame-level shared feature of an utterance as a single dot and colorized it according to the system to which the utterance belongs.

For the VCC'18, we consider two systems made by one team as one system since they have similar characteristics, resulting in 26 systems. Then for both test data, we sort the systems in descending order according to the system-level MOS and evenly select half of them. The red indicates the source speech ('S00' or 'SRC'), and the orange indicates the spoofing system with the highest MOS ('N10' or 'N'). We randomly select 390 and 300 utterances among the VCC'18 and 16 data, respectively, so that each system has an average of 15 utterances.

The *concentrating effect* can be easily observed from red and orange dots in (a) and (b), where those points are more closely together in +SD. In (e), the colors except the red tend to be more mingled with other colors and less cohesive than in (d). This indicates the *ignoring effect*. (d), (e), and (f) clearly shows the ability of STC to distinguish between the systems. Compared to (a), (b), and (c), the points are more clustered according to their classes. The effect of the FL (i.e., keeping the *concentrating effect* and alleviating the *ignoring effect*) can be observed by comparison between (b) and (c) or (e) and (f).

5. Conclusion

We proposed MTL with SD and STC to improve the deep MOS predictor. With experimental results on the VCC'18 and VCC'16 evaluation data, we showed that both the SD and STC tasks improve MOS prediction. Furthermore, we adopt the FL to maximize the synergy between the two tasks. The proposed MTL model can be used to automatically evaluate and compare several speech generation systems. For future work, we will consider the ranks of the utterance-level MOSs to increase the SRCC. By providing the MOS predicted by our proposed model, we will also directly guide a speech generation model to synthesize speech with high MOS as well as low MSE.

6. Acknowledgements

This material is based upon work supported by the Ministry of Trade, Industry & Energy (MOTIE, Korea) under Industrial Technology Innovation Program (No. 10080667, Development of conversational speech synthesis technology to express emotion and personality of robots through sound source diversification).

7. References

- [1] A. Oord, S. Dieleman, H. Zen, K. Simonyan, O. Vinyals, A. Graves, N. Kalchbrenner, A. Senior, and K. Kavukcuoglu, “WaveNet: A generative model for raw audio,” *arXiv preprint arXiv:1609.03499*, 2016.
- [2] J. Shen, R. Pang, R. J. Weiss, M. Schuster, N. Jaitly, Z. Yang, Z. Chen, Y. Zhang, Y. Wang, R. Skerry-Ryan, R. A. Saurous, Y. Agiomyrgiannakis, and Y. Wu, “Natural TTS synthesis by conditioning WaveNet on Mel spectrogram predictions,” in *Proc. of the IEEE International Conference on Acoustics, Speech and Signal Processing (ICASSP)*, 2018, pp. 4779–4783.
- [3] W. Ping, K. Peng, A. Gibiansky, S. O. Arik, A. Kannan, S. Narang, J. Raiman, and J. Miller, “Deep Voice 3: Scaling text-to-speech with convolutional sequence learning,” in *Proc. of the International Conference on Learning Representations (ICLR)*, 2018.
- [4] N. Li, S. Liu, Y. Liu, S. Zhao, and M. Liu, “Neural speech synthesis with Transformer network,” in *Proc. of the AAAI Conference on Artificial Intelligence*, 2019, pp. 6706–6713.
- [5] T. Kaneko and H. Kameoka, “CycleGAN-VC: Non-parallel voice conversion using cycle-consistent adversarial networks,” in *Proc. of 2018 26th European Signal Processing Conference (EUSIPCO)*, 2018, pp. 2100–2104.
- [6] M. Chu and H. Peng, “An objective measure for estimating MOS of synthesized speech,” in *Proc. of Eurospeech*, 2001.
- [7] T. Yoshimura, G. E. Henter, O. Watts, M. Wester, J. Yamagishi, and K. Tokuda, “A hierarchical predictor of synthetic speech naturalness using neural networks,” in *Proc. of Interspeech*, 2016, pp. 342–346.
- [8] B. Patton, Y. Agiomyrgiannakis, M. Terry, K. W. Wilson, R. A. Saurous, and D. Sculley, “AutoMOS: Learning a non-intrusive assessor of naturalness-of-speech,” in *Proc. of NIPS End-to-end Learning for Speech and Audio Processing Workshop*, 2016.
- [9] C. Lo, S. Fu, W. Huang, X. Wang, J. Yamagishi, Y. Tsao, and H. Wang, “MOSNet: Deep learning based objective assessment for voice conversion,” in *Proc. of Interspeech*, 2019, pp. 1541–1545.
- [10] R. A. Caruana, “Multitask learning: A knowledge-based source of inductive bias,” in *Proc. of the international conference on machine learning (ICML)*, 1993.
- [11] S. Ruder, “An overview of multi-task learning in deep neural networks,” *arXiv preprint arXiv:1706.05098*, 2017.
- [12] S. Subramanian, A. Trischler, Y. Bengio, and C. J. Pal, “Learning general purpose distributed sentence representations via large scale multi-task learning,” in *Proc. of the International Conference on Learning Representations (ICLR)*, 2018.
- [13] R. Girshick, “Fast R-CNN,” in *Proc. of the IEEE International Conference on Computer Vision (ICCV)*, 2015, pp. 1440–1448.
- [14] S. Toshniwal, H. Tang, L. Lu, and K. Livescu, “Multitask learning with low-level auxiliary tasks for encoder-decoder based speech recognition,” in *Proc. of Interspeech*, 2017.
- [15] T. Maekaku, Y. Kida, and A. Sugiyama, “Simultaneous detection and localization of a wake-up word using multi-task learning of the duration and endpoint,” in *Proc. of Interspeech*, 2019, pp. 4240–4244.
- [16] L. You, W. Guo, L. Dai, and J. Du, “Multi-task learning with high-order statistics for x-vector based text-independent speaker verification,” in *Proc. of Interspeech*, 2019, pp. 1158–1162.
- [17] A. Jati, R. Peri, M. Pal, T. J. Park, N. Kumar, R. Travadi, P. Georgiou, and S. Narayanan, “Multi-task training of hybrid DNN-TVM model for speaker verification with noisy and far-field speech,” in *Proc. of Interspeech*, 2019, pp. 2463–2467.
- [18] J. Bingel and A. Søggard, “Identifying beneficial task relations for multi-task learning in deep neural networks,” *arXiv preprint arXiv:1702.08303*, 2017.
- [19] S. Louvan and B. Magnini, “Exploring named entity recognition as an auxiliary task for slot filling in conversational language understanding,” in *Proc. of the 2018 EMNLP Workshop on Search-Oriented Conversational AI (SCAI)*, 2018, pp. 74–80.
- [20] T. Y. Lin, P. Goyal, R. Girshick, K. He, and P. Dollr, “Focal loss for dense object detection,” in *Proc. of the IEEE international conference on computer vision (ICCV)*, 2017, pp. 2980–2988.
- [21] P. L. De Leon, I. Hernaez, I. Saratzaga, M. Pucher, and J. Yamagishi, “Detection of synthetic speech for the problem of imposture,” in *Proc. of the IEEE International Conference on Acoustics, Speech and Signal Processing (ICASSP)*, 2011, pp. 4844–4847.
- [22] J. Lorenzo-Trueba, J. Yamagishi, T. Toda, D. Saito, F. Villavicencio, T. Kinnunen, and Z. Ling, “The voice conversion challenge 2018: Promoting development of parallel and nonparallel methods,” in *Proc. of Odyssey The Speaker and Language Recognition Workshop*, 2018, pp. 195–202.
- [23] T. Toda, L. Chen, D. Saito, F. Villavicencio, M. Wester, Z. Wu, and J. Yamagishi, “The Voice Conversion Challenge 2016,” in *Proc. of Interspeech*, 2016, pp. 1632–1636.
- [24] K. Pearson, “Notes on the history of correlation,” *Biometrika*, vol. 13, no. 1, pp. 25–45, 1920.
- [25] C. Spearman, “The proof and measurement of association between two things,” *The American Journal of Psychology*, vol. 15, no. 1, pp. 72–101, 1904.
- [26] L. V. D. Maaten and G. Hinton, “Visualizing data using t-SNE,” *Journal of machine learning research*, no. 9, pp. 2579–2605, 2008.